

**HHS PUBLIC ACCESS**

Author manuscript

*Can J Cardiol.* Author manuscript; available in PMC 2016 April 01.

Published in final edited form as:

*Can J Cardiol.* 2015 April ; 31(4): 391–406. doi:10.1016/j.cjca.2015.01.023.

## Right Ventricular Adaptation and Failure in Pulmonary Arterial Hypertension

John J. Ryan, MD<sup>1</sup>, Jessica Huston, MD<sup>2</sup>, Shelby Kutty, MD<sup>3</sup>, Nathan D. Hatton, MD<sup>4</sup>, Lindsay Bowman, BMSc<sup>5</sup>, Lian Tian, PhD<sup>5</sup>, Julia E. Herr, MSc<sup>5</sup>, Amer M. Johri, MD, MSc<sup>5</sup>, and Stephen L. Archer, MD<sup>5</sup>

<sup>1</sup>Division of Cardiovascular Medicine, Department of Medicine, University of Utah, Salt Lake City, UT, United States

<sup>2</sup>Department of Medicine, University of Utah, Salt Lake City, UT, United States

<sup>3</sup>Pediatric Cardiology, University of Nebraska Medical Center, Children's Hospital and Medical Center, Omaha, NE, United States

<sup>4</sup>Division of Pulmonary Medicine, Department of Medicine, University of Utah, Salt Lake City, UT, United States

<sup>5</sup>Department of Medicine, Queen's University, Kingston, Ontario, Canada

### Abstract

Pulmonary arterial hypertension (PAH) is an obstructive pulmonary vasculopathy, characterized by excess proliferation, apoptosis-resistance, inflammation, fibrosis and vasoconstriction. While PAH therapies target some of these vascular abnormalities (primarily vasoconstriction) most do not directly benefit the right ventricle (RV). This is suboptimal since a patient's functional state and prognosis are largely determined by the success of the adaptation of the RV to the increased afterload. The RV initially hypertrophies but may ultimately decompensate, becoming dilated, hypokinetic and fibrotic. A number of pathophysiologic abnormalities have been identified in the PAH RV, including: ischemia and hibernation (partially reflecting RV capillary rarefaction), autonomic activation (due to GRK2-mediated down-regulation and desensitization of  $\beta$ -adrenergic receptors), mitochondrial-metabolic abnormalities (notably increased uncoupled glycolysis and glutaminolysis), and fibrosis. Many RV abnormalities are detectable by molecular imaging and may serve as biomarkers. Some molecular pathways, such as those regulating angiogenesis, metabolism and mitochondrial dynamics, are similarly deranged in the RV and pulmonary vasculature, offering the possibility of therapies that treat both the RV and pulmonary circulation. An important paradigm in PAH is that the RV and pulmonary circulation constitute a unified

© 2015 Canadian Cardiovascular Society.

**Address for correspondence:** Stephen L. Archer MD, FRCP(C), FAHA, FACC, Professor and Head, Department of Medicine, Queen's University, Etherington Hall, Room 3041, 94 Stuart St., Kingston, Ontario, Canada, K7L 3N6, stephen.archer@queensu.ca, Telephone: 613 533-6327, Fax: 613 533-6695.

**Publisher's Disclaimer:** This is a PDF file of an unedited manuscript that has been accepted for publication. As a service to our customers we are providing this early version of the manuscript. The manuscript will undergo copyediting, typesetting, and review of the resulting proof before it is published in its final citable form. Please note that during the production process errors may be discovered which could affect the content, and all legal disclaimers that apply to the journal pertain.

cardiopulmonary unit. Clinical trials of PAH pharmacotherapies should assess both components of the cardiopulmonary unit.

### Keywords

Warburg effect; Randle cycle; pyruvate dehydrogenase kinase; dynamin related protein-1 (DRP1); dichloroacetate; trimetazidine; ranolazine; glucose oxidation; mitofusin-2; right ventricular failure; fatty acid oxidation; WHO Group 1 pulmonary hypertension (PAH); glutaminolysis; fluorodeoxyglucose positron emission tomography (PET) ( $^{18}\text{F}$ -FDG PET)

### Introduction

Pulmonary Arterial Hypertension (PAH) is a pulmonary vasculopathy defined by a resting mean pulmonary artery pressure (mPAP)  $>25$  mmHg and pulmonary capillary wedge pressure (PCWP)  $<15$  mmHg<sup>1</sup>. Right ventricular (RV) function is a major determinant of prognosis and functional capacity in PAH<sup>2-4</sup>. RV failure in PAH reflects maladaptive responses to the increased afterload that defines PAH (pulmonary vascular resistance, PVR,  $> 3$  Wood units). RV failure requiring admission to an intensive care unit and inotropic support has an inpatient mortality rate of over 40%<sup>5</sup>. Approaches to the support of the failing RV varies considerably among providers and centers<sup>5,6</sup> and limited interventional options are currently available for RV failure<sup>7</sup>. There are currently no official guidelines for the treatment of RV failure in PAH, due to the lack of effective, evidence-based therapies<sup>8</sup>. A National Heart Lung and Blood Institute-sponsored working group has highlighted the need to develop a basic understanding of the unique properties of the RV, in order to advance the understanding and therapy of RV failure in PAH<sup>9</sup>. Among the important features that may lead to RV failure in pulmonary hypertension (PH) are: (a) the RV's limited contractile reserve which, despite hypertrophy, limits capacity for adaptation to an elevation of the transpulmonary gradient<sup>10</sup>; (b) ischemia due to reduced perfusion pressure of the right coronary artery (RCA), as increasing PAP decreases the aorta-RV pressure gradient thereby reducing epicardial systolic flow<sup>11</sup> and/or microvascular rarefaction in the RV<sup>11,12</sup> (c) a metabolic shift from oxidative mitochondrial metabolism to the energetically inefficient cytosolic process of aerobic glycolysis<sup>12,13</sup>; and (d)  $\beta$ -adrenoreceptor down-regulation and desensitization<sup>14</sup>.

Approved PAH therapies do not directly target the RV and their effects on RV contractility are largely unknown, since they have been approved based primarily on their ability to improve 6-minute walk test distance (6MWD). Even in PAH patients who experience a decrease in PVR in response to pulmonary vasodilators, RV function can deteriorate<sup>15</sup>. In this review, we will discuss the clinical, pathophysiological and therapeutic features of RV failure and discuss future directions for RV research, indicating potential therapeutic strategies (Figure 1).

### Clinical features of RV failure

RV failure reflects the inability of the RV to perfuse the lung circulation adequately to ensure LV filling while maintaining normal diastolic pressures. RV failure is characterized

by a decreased cardiac index ( $< 2.5 \text{ L/min/m}^2$ ) and increased right-sided, cardiac filling pressures, including right atrial pressure (RAP)  $\geq 8 \text{ mmHg}$ <sup>16</sup>.

RV failure in PAH causes pedal edema, neck vein distension, abdominal fullness and exertional dyspnea (which portends poor survival<sup>17</sup>). Palpitations due to supraventricular tachycardia occur in 12% of PAH patients and reflect the progressive anatomical distortion and enlargement of the RV and right atrium<sup>18,19</sup>. Presyncope and syncope occur in ~4% of PAH patients and indicate a poor prognosis<sup>20</sup>. Exertional syncope is particularly common in PAH and reflects the RV's inability to overcome the fixed pulmonary vascular obstruction and increase cardiac output in the face of systemic vasodilatation.

On physical examination, the signs of RV failure include an increase in jugular venous pressure (JVP), often associated with a prominent v-wave, due to severe tricuspid regurgitation (Video 1), dependent edema and hepatic congestion<sup>2</sup>. Carvallo's sign (increase in volume of tricuspid regurgitation murmurs during inspiration) distinguishes this systolic murmur from mitral regurgitation<sup>21</sup>. Precordial palpation may reveal an RV lift or heave, indicating RV enlargement. Auscultation in the tricuspid area sometimes reveals a right-sided third heart sound (S<sub>3</sub>), reflective of a failing and non-compliant RV. A high-pitched early diastolic murmur reflecting pulmonary regurgitation (the Graham Steell murmur) may occur in RV failure<sup>22</sup>. Maneuvers that increase venous return may expose the signs of RV failure in patients who are euvolemic or hypovolemic. These maneuvers include hepatojugular reflux, characterized by a sustained rise in JVP of 4 cm upon 15-30 seconds pressure over the liver<sup>23</sup>, and Kussmaul's sign, in which the JVP increases with inspiration, rather than the normal decline.

The lateral chest radiograph (CXR) often reveals RV enlargement, evident as a loss of the retrosternal space and the posterior-anterior CXR shows evidence of RV and right atrial (RA) enlargement. In addition, by the stage when there is RV failure the CXR may also show pruning of the vasculature (Figure 1, Panel A). The electrocardiogram (ECG) patterns in patients with PAH includes sinus rhythm or sinus tachycardia with right atrial enlargement (P-pulmonale), right axis deviation ( $> 90$  degrees), an early R-wave transition (R/S ratio  $> 1$  in lead V<sub>1</sub>), a right bundle branch block and/or an RV strain pattern, evident as the S<sub>1</sub>Q<sub>3</sub>T<sub>3</sub> pattern (Figure 2). In patients with RV failure there is often T-wave inversion in leads V1-3, consistent with RV strain.

Although the physical examination is helpful, advanced cardiac imaging and invasive hemodynamic measurements are required to solidify the diagnosis of PAH and assess RV failure. Invasive hemodynamics should always precede initiation of PAH-specific therapy.

## RV Imaging in PAH

Chronic RV pressure overload in PAH can induce RV hypertrophy (RVH), which may initially be adaptive; however over time concentric RVH with preserved RV function can evolve to RV dilatation and systolic dysfunction (Figure 1, Panel B).

## Echocardiography

Traditionally echocardiographic evaluation of the RV is difficult, due to the crescentic shape, which confounds modeling of simple geometric estimation of volume by 2-dimensional methods<sup>24</sup>; however, the recent application of real-time 3-dimensional echocardiography has improved the ability to use ultrasound to serially monitor RV function<sup>25</sup>. Many echocardiographic RV parameters predict prognosis in PAH (Table 2), including RVH, defined as an end-diastolic free-wall thickness > 5mm<sup>26</sup>, reflecting an increase in RV mass<sup>27</sup>. In addition to RVH, RV pressure overload results in septal flattening and bowing that compresses the LV into a “D-shape”<sup>24</sup>. Over time, RV contractile dysfunction is accompanied by RV dilatation in decompensated patients. RV dilatation is traditionally best visualized in the apical 4 chamber view and is defined as an RV diameter greater than 42 mm at the base, greater than 35mm at mid-level, or a longitudinal measurement of greater than 86 mm<sup>26</sup>. The RV fractional area of change (FAC) is defined as the percentage of change in the RV chamber area between systole and diastole<sup>28</sup>. FAC of less than 35% indicates RV dysfunction<sup>24</sup>. Unlike the LV, much of the RV ejection fraction (RVEF) results from longitudinal shortening, which can be measured using M-mode by monitoring the excursion of the tricuspid annulus. Tricuspid annular plane systolic excursion (TAPSE) assesses the RV’s longitudinal shortening and is a reliable predictor of prognosis in adults with PAH. TAPSE varies inversely with RVEF and a TAPSE of <18 mm predicts increased mortality<sup>29</sup>. The RV-myocardial performance index (RV-MPI or Tei index), incorporates elements of both systolic and diastolic phases to assess global ventricular function. The RV-MPI index is defined as the ratio of isovolemic time divided by ejection time (ET), or [(Isovolemic relaxation time + Isovolemic contraction time)/ET]<sup>26</sup>. RV dysfunction is defined by MPI values of > 0.40 by pulsed wave Doppler and > 0.55 by tissue Doppler<sup>24</sup>. Systolic longitudinal RV myocardial contractility is recorded as peak systolic tricuspid lateral annular velocity (S’), measured by pulsed Doppler tissue imaging of the tricuspid annulus. An S’ of < 9.7 cm/sec is associated with abnormal RV contractility<sup>30</sup>.

More recently, speckle tracking has been used to analyze RV mechanics and derive RV deformation indices (strain and strain rate). Speckle tracking, or deformation analysis, has been shown to accurately assess RV function in PAH patients and has the advantage of not being angle-dependent within the imaging plane<sup>31,32</sup>. Speckle tracking, as a non-invasive mode of RV assessment, has been shown to predict mortality in PAH<sup>33</sup>. Strain is measured in negative percentage with larger negative numbers representing greater amounts of strain<sup>34</sup>. In PAH, RV free wall strain values less (more negative) than –12.5% correlate with greater disease progression at six months, as measured by symptoms and WHO functional class<sup>33</sup>. In a study of Group I-V PH patients, RV longitudinal peak systolic strain (LPSS) less than –19% was associated with three times higher mortality than those patients with RVLPS more than –19%. In this study, each 1% decrease in RVLPS below –19% was associated with a 13% increase in risk of death (Table 2)<sup>35</sup>. However, speckle tracking is not universally available and, because of important differences in algorithms used by different vendors, is not standardized. Consequently there are not yet platform-independent diagnostic criteria or universal normal values for speckle tracking in PAH<sup>26</sup>. Nonetheless, strain evaluation by speckle tracking echocardiography is a promising technology for non-invasive

evaluation of RV function and will likely gain similar clinical acceptance as has occurred with left ventricular strain echocardiography.

### Cardiac MRI

Cardiac MRI is the gold-standard for measuring RV size, function, flow<sup>36</sup> and mass<sup>36</sup>. RV functional evaluation by cardiac MRI is highly reproducible, permitting serial tracking of RV function<sup>37</sup>. Cardiac MRI is also ideally suited for RV assessments in clinical trials of PAH therapies, since its high reproducibility allows detection of modest changes in RVEF with small sample size studies<sup>25</sup>. MRI measures of low stroke volume, RV dilatation, and impaired RV filling are each independent predictors of mortality in PAH<sup>38</sup>. Reduced survival was seen in patients with RV stroke volume index  $< 25 \text{ mL/m}^2$ , a RV end-diastolic volume index (RVEDVI) greater than  $84 \text{ mL/m}^2$ , and a LV end diastolic volume less than  $40 \text{ mL/m}^2$ <sup>38</sup>. More recently, an increased RV end systolic volume has been shown to correlate with increased mortality<sup>39</sup>. A complete cardiac MRI study in a PAH patient should include measure of RV mass, volume and RVEF as well as phase contrast mapping (to measure pulmonary blood flow and PA acceleration time) and infusion of gadolinium (to detect late gadolinium myocardial enhancement, LGE). LGE reflects myocardial fibrosis and the presence of LGE at the septal hinge points of the RV is a powerful predictor of adverse outcomes<sup>40</sup>. RV mass and end-diastolic wall thickness<sup>41,42</sup> and the LV septal-to-free wall curvature ratio<sup>43</sup> each correlate well with mPAP. Tagged MRI can be used to measure segmental RV motion in a three-dimensional manner and identifies significant interventricular dyssynchrony in PAH due to RVH and delayed RV conduction<sup>44,45</sup>. Features of RV adaptation and failure detectable on MRI are summarized in Table 3.

### Right heart catheterization

Right heart catheterization (RHC) remains necessary for the definitive diagnosis of PAH and follow-up RHC can demonstrate the presence or absence of RV failure. The key measurements in RHC are RAP, mPAP, PCWP and cardiac output/index, the latter two in particular are reflective of RV failure<sup>9</sup>. In the evaluation of PAH, hemodynamics should be performed in centers where there is sufficient expertise, as there are continued complexities in this field.

Another hemodynamic features of RV failure in end-stage PAH include a decline in mPAP; as RAP increases, the failing RV is unable to compensate for the increased RV afterload<sup>46</sup>. One feature of worsened prognosis in left sided heart failure is Kussmaul sign, a paradoxical rise in right atrial pressure during inspiration<sup>47</sup>. This increase in RA pressure is thought to be secondary to an increased preload in a non-compliant right ventricle<sup>48</sup>. In patients with HFrEF evaluated for cardiac transplantation, Kussmaul physiology correlated with increased RA pressures, mPAP and PCWP<sup>49</sup>. In patients who received cardiac transplants, 80% of those with Kussmaul physiology had post-transplant RV failure and those with Kussmaul physiology had a significantly higher risk of pre-transplant death or need for a ventricular assist device, as well as, post-transplant death or RV failure<sup>49</sup>.

For hemodynamic measurements, it is also important to record these measurements at end-expiration. Operator review of the pressure tracings is required to avoid computer error,

which in particular can significantly underestimate PCWP - the very measurement upon which the differentiation of Group 1 *versus* Group 2 PH depends<sup>1,50</sup>. More recently, however, the recommendation of end-expiratory measurements of PCWP has been challenged because it can result in false increased estimations of mPAP and PCWP<sup>51</sup>.

More refined measurements can be made with micromanometer PA catheters. These catheters have a pressure transducer mounted on the tip of the catheter and are considerably more accurate due to the avoidance of many of the sources of error that characterize the standard balloon-flotation catheters. The pressure waveform obtained from these catheters is more precise and there is no delay in obtaining the waveform, unlike the 40 millisecond delay seen with the fluid-filled catheter system. These catheters also allow for the measurement of ventricular contractility (dP/dT), ventricular pressure delay (-dP/dT), ventricular relaxation (tau constant), wall stress and ventricular pressure-volume relationships<sup>52</sup>. However, the disadvantage of these micromanometer catheters is that they are rigid, not balloon-guided, fragile, more expensive, more time-consuming to use and also require advanced calibration and operator skill. Ideally a complete hemodynamic assessment of a PAH patient should include a left heart catheterization with measurement of the LVEDP.

### Nuclear Imaging

Nuclear imaging also plays a role in assessing RV function and adaptation in PAH (Figure 3), however much of its use remains investigational and hypothesis-generating. Depending on the radiotracer used, single proton emission computed tomography (SPECT) permits detection of RV ischemia<sup>11,53</sup> and changes in adrenergic activation. Positron emission tomography (PET), and hybrid studies with SPECT/CT and PET/CT are invaluable in measuring RV metabolism and perfusion *in vivo* and permit simultaneous co-registration of biochemical and anatomic or functional information. RVH, with increased chamber mass and coronary blood flow, augments radiotracer delivery, making it possible to image the RV, which is often not possible in patients who lack RVH<sup>45</sup>. In PAH there is evidence of RV ischemia (reduced flow reserve)<sup>54</sup>. This ischemia may reflect both reduced RCA blood flow during systole (due to a decrease in the driving gradient which occurs as RV systolic pressure approaches aortic systolic pressure)<sup>55</sup>, and impaired angiogenesis and capillary rarefaction<sup>56,57</sup>.

<sup>123</sup>I-Metaiodobenzylguanidine (MIBG) imaging is used to evaluate the cardiac autonomic nervous system<sup>58</sup>. MIBG is a norepinephrine analog. Plasma norepinephrine levels are increased in PAH, predicting poorer survival and worse functional class<sup>59</sup>. In PAH and CTEPH, MIBG uptake in the left ventricle is decreased and its rate of washout increased<sup>60</sup>. Additionally, PH patients with lower left ventricular MIBG uptake, as represented by a heart to mediastinum ratio < 2.0 have significantly higher mortality<sup>60</sup>. This reflects adrenergic activation and downregulation of the  $\beta$ -adrenoreceptors that accompanies RV in PAH<sup>61</sup>. MIBG imaging in the RV has great potential value in PAH and remains under active investigation.

Much of the current understanding of RV failure has been derived from studies of left ventricular systolic heart failure populations. Left heart failure with reduced ejection fraction

(HFrEF) produces a congestive pulmonary venous hypertension that can lead to RV dysfunction<sup>62</sup>. PH with RV failure in HFrEF population is associated with poor prognosis and increased mortality<sup>63,64</sup>. RV dysfunction in left heart failure with preserved ejection fraction (HFpEF) is less well characterized. The prevalence of RV dysfunction in HFpEF was previously estimated between 33-50%<sup>65</sup>; however, more recent data suggests a lower prevalence (21-35%)<sup>66</sup>. RV dysfunction, in HFpEF is associated with decreased overall survival, increased cardiovascular mortality and increased heart failure hospitalizations<sup>66</sup>. Although studies of HFrEF and HFpEF are informative, the RV in PAH is likely afflicted by chamber-specific abnormalities that are unique to PAH. Thus RVH and RV failure in PAH is likely to be a valuable independent research topic that is not a simple extension of studies of LVH and LV failure.

### Adaptive versus maladaptive RVH

There is debate about the benefit of RVH in PAH. Increased RV mass can compensate in part for increased PVR and helps maintain cardiac output in PAH. However, there is heterogeneity in the type of RVH seen in PAH and the severity of the hypertrophic response may be considered as being adaptive or maladaptive. Some patients with PAH remain well-compensated whilst others with identical hemodynamic stress rapidly develop RV failure. The effect of RVH on cardiac output and the likelihood of progression to RV failure are unpredictable<sup>11</sup>. Some patients have adaptive forms of RVH and remain clinically stable with preserved cardiac output for decades, whereas despite similar elevations in RV pressure and RVH, others have maladaptive forms of RVH and rapidly decompensate<sup>13</sup>. Of note, patients with pulmonic stenosis, who have RV pressure overload without concomitant pulmonary vascular disease, often have concentric RVH with preserved RV function for many decades<sup>67-69</sup>. Even within Group 1 PAH, RV failure is much more prevalent in patients with scleroderma-associated PAH<sup>70,71</sup>, than in those whose PAH is associated with congenital heart disease, such as patients who develop Eisenmenger's syndrome<sup>72</sup>. The type of RVH seen in scleroderma PAH may be considered maladaptive, whilst that in Eisenmenger's syndrome is (relatively) adaptive, although the definition of these two states is imperfect and clinically a spectrum exists. Molecular features of adaptive and maladaptive RVH have recently been reviewed<sup>2</sup>.

Maladaptive RVH commonly displays RV fibrosis and dilatation. The maladaptive phenotype is characterized by reduced exercise capacity, significant reductions in RVEF, and decreased cardiac output<sup>16</sup>. In contrast, adaptive RVH is characterized by concentric hypertrophy with minimal RV dilatation or fibrosis, with preservation of exercise capacity, RVEF, and cardiac output<sup>73</sup>. There are many factors that determine whether RVH will be well tolerated, including the severity of metabolic changes, ischemia, fibrosis, and autonomic dysregulation. Many of these factors are epigenetically modified or regulated by RV-specific activation of transcription factors such as Hypoxia Inducible Factor-1 $\alpha$  (HIF-1 $\alpha$ ), cMyc and FOXO-1<sup>74-76</sup>. Rodent models of RVH recapitulate the division of RVH into adaptive and maladaptive types. In these models it is clear that the heterogeneity is not fully explained by differences in RV mass or severity of the RV pressure overload<sup>12</sup>. For example, rodents with pulmonary artery banding (PAB) have preserved survival and better

functional capacity, relative to rats with RVH induced by monocrotaline or chronic hypoxia + SU5416<sup>77</sup>, despite identical RV mass and RV systolic pressure.

Ultimately coronary perfusion may fail to meet the increased demands for oxygen in RVH; leading to RV ischemia which, in turn, leads to RV failure<sup>78</sup>. RV ischemia in PAH may result from capillary rarefaction and/or a decrease in right coronary artery perfusion pressure<sup>11</sup> (Figure 5).

In RVH, an increase in mitochondrial-derived reactive oxygen species (ROS) can potentially result in inhibition of HIF-1 $\alpha$  thereby suppressing angiogenesis<sup>11</sup>. This decrease in angiogenesis can result in ischemia and contribute to the rapid deterioration of RV function in maladaptive RVH<sup>79</sup>. Capillary rarefaction is defined as a decrease in the density of capillaries and small intramyocardial arterioles in the RV<sup>80</sup>, and is particularly common in patients with scleroderma-associated PAH<sup>81</sup> and in rodent models induced by monocrotaline. It is noteworthy that in animal models of PAH, the PAH-inducing stimuli are endothelial toxins (e.g. monocrotaline, SU5416). Perhaps anti-angiogenic or endothelial toxins may directly reduce RV microvasculature while simultaneously eliciting pulmonary vascular disease. This is a different concept than the notion that RV capillary rarefaction is the result of increased PVR and RVH, which secondarily activates anti-angiogenic pathways.

RV ischemia in PAH may also reflect impaired epicardial coronary perfusion. In normal individuals, the RCA fills in both systole and diastole, secondary to low RV systolic pressure (RVSP). In the setting of RV pressure overload, the difference between aortic systolic pressure and RVSP (the systolic perfusion gradient) may be eliminated, (reducing systolic RCA flow). Moreover, the pressure difference between aortic and RV diastolic pressures (i.e. diastolic perfusion pressure) may also be reduced, thereby impairing RCA flow in diastole<sup>82,83</sup>. When the RCA perfusion pressure falls below 50 mmHg, RV contractile function declines<sup>84</sup>.

## Metabolism

In PAH, mitochondrial metabolism is actively and reversibly suppressed<sup>85</sup>. In PAH, the RV undergoes a number of metabolic changes, including an increased reliance on glycolysis, not coupled to glucose oxidation, which yields lactate. The shift to the less energetically efficient process of glycolysis results in a compensatory upregulation of glucose flux into RV myocytes that can be quantified using <sup>18</sup>FDG PET scans<sup>80,86</sup>. This uncoupled glycolysis is much less energy efficient than is glycolysis that is coupled to glucose oxidation<sup>79</sup>. Uncoupled glycolysis generates only 2 mole of ATP per 6-carbon glucose *versus* 36 mole of ATP with a coupled glycolytic-oxidative pathway. To support this inefficient metabolism glucose influx via the glut transporters is increased, whether triggered by ischemia and/or by transcriptional changes in RV myocytes. This can be detected noninvasively using positron emission tomographic (PET) quantification of the uptake of <sup>18</sup>fluorodeoxyglucose (<sup>18</sup>FDG), a glucose analog, which is taken up into the myocyte via the Glut transporter, but does not undergo metabolism<sup>18</sup>. Thus, measuring <sup>18</sup>FDG PET accurately reflects glucose uptake and glycolysis but does not always predict downstream metabolism, since increased glucose



uptake can reflect with increased uncoupled glycolysis (as occurs with ischemia) or increased glycolysis that is coupled to glucose oxidation.

Increased RV uptake of  $^{18}\text{F}$ FDG has been demonstrated in PAH patients and is reversible with effective PAH therapy (even when the therapy is not directly metabolically targeted)<sup>87</sup> (Figure 3). Similar increases in RV uptake of  $^{18}\text{F}$ FDG occur in rodent models of PAH and in these models, expression of the glucose transporter, Glut-1, is increased. In humans and rodents with PAH, a common mechanism of this metabolic switch involves transcriptional upregulation of pyruvate dehydrogenase kinase (PDK)<sup>13</sup> in the RV. PDK exists in 4 isoforms, of which PDK2 and PDK4 are predominant in the RV. PDK phosphorylates and inhibits pyruvate dehydrogenase (PDH), the major enzyme complex in the mitochondria responsible for glucose oxidation. Increased PDK activity/expression in RVH is an acquired abnormality, but ultimately compromises RV energetics and contributes to RV hypokinesia. PDK4 expression is increased in the RV of both animal models of PAH and PAH patients<sup>57</sup>.

The maladaptive reliance on uncoupled glycolysis in RVH can therapeutically be reversed by inhibition of PDK, using dichloroacetate (DCA). DCA is an inhibitor of all 4 PDK isoforms and when administered in the RV working heart model it increases cardiac output within 40 minutes<sup>77</sup>. Longer term oral DCA (1-month to 1-year), improves RV function in several models of PAH *in vivo*, including chronic hypoxic pulmonary hypertension<sup>88,89</sup>, monocrotaline-PAH<sup>88</sup>, and spontaneous PAH in Fawn-hooded rats<sup>90</sup> (Figure 4). The benefits of DCA reflect its ability to both regress pulmonary vascular disease and to improve RV contractility. However, PDK inhibition in RVH is beneficial in the absence of pulmonary vascular disease. For example, DCA increases cardiac output even in a PAB RVH model, in which there is fixed RV obstruction. However, the benefits of DCA in PAB are qualitatively less than those seen in PAH models, in which benefits derive both from effects on the lung vasculature and RV<sup>73,77</sup>. PDK-PDH is a therapeutic target shared throughout the cardiopulmonary unit. DCA is the subject of a recently completed clinical trial (Clinical Trials: NCT01083524)<sup>88,91</sup>. This is a phase 1 study involving up to 30 patients with PAH in two centers. The primary outcome after 16 weeks of DCA treatment is safety and tolerability of DCA. Secondary outcomes include functional capacity, PVR, MRI measurements of RV,  $^{18}\text{F}$ FDG uptake in the lung and RV, among other outcomes. The study has been completed but the results are not yet available.

The use of PDK inhibitors allows for reactivation of PDH in minutes and over days increases PDH expression<sup>77</sup>. However, there are other strategies by which glucose oxidation can be restored. One such strategy exploits the Randle cycle, the reciprocal relationship between glucose oxidation and fatty acid oxidation (FAO)<sup>73,92</sup>. FAO suppresses glucose oxidation leading to aerobic glycolysis and accumulation of lactate, which requires various energy-dependent pumps to maintain pH balance. Thus, FAO consumes 12% more oxygen per mole of ATP produced than does glucose oxidation<sup>87</sup>. In RVH, with reduced RCA perfusion pressure and microvascular rarefaction, there may be inadequate oxygen to support FAO. In one study, FAO inhibitors were orally administered to prevent RVH (trimetazidine, 0.7 g/L for 8 weeks) or regress RVH (ranolazine 20 mg/day or trimetazidine for 1 week, beginning 3 weeks after pulmonary artery banding). Metabolic, molecular, ECG, functional, and hemodynamic comparisons with sham rats were performed 4 or 8 weeks

after PAB and therapeutic benefit was observed (increased cardiac output, increased treadmill exercise time). These FAO inhibitors increased treadmill exercise capacity and cardiac output<sup>73,75</sup>. A clinical trial studying the effects of FAO inhibitors on patients with PAH is ongoing<sup>93,94</sup>.

Recently, RVH was associated with induction of RV glutaminolysis. Like aerobic glycolysis, glutaminolysis is a form of metabolism which permits rapid cell growth<sup>95</sup>. Glutaminolysis is classically associated with cancer cells. In the RV, it appears that glutaminolysis results from activation of the proto-oncogene cMyc, which reactivates this and many other components of the fetal gene package<sup>12,57</sup>. Glutaminolysis is absent from the normal RV, but is induced selectively in RVH<sup>12</sup>. In a single study in rodents, inhibition of glutaminolysis enhances glucose oxidation and improves RV function. This reciprocal interaction between metabolic pathways is analogous to the effects of FAO inhibitors on glucose oxidation in the Randle cycle. Early therapeutic trials with the glutaminolysis inhibitor 6-Diazo-5-oxo-L-norleucine (DON, a norleucine analog) demonstrate beneficial effects on RV function and a reduction in RVH. However, DON causes unacceptable levels of gastrointestinal toxicity and muscle wasting, problems that were seen when similar agents were used in cancer patients<sup>96</sup>.

### Sympathetic activation

PAH patients with RV failure have high circulating catecholamine levels and lose the normal ability to augment catecholamine levels with exercise<sup>97</sup>. They also have impaired inotropic response to  $\beta$ -adrenergic receptor agonists, reflecting receptor downregulation and desensitization. These changes are restricted to the RV when RVH is adaptive (e.g. PAB)<sup>14</sup>, but may also affect the LV in circumstances of maladaptive RVH, (e.g. in monocrotaline or chronic hypoxia-SU5416-induced PAH)<sup>14,98,99</sup>. In maladaptive RVH there is a broad downregulation of most adrenoreceptors in RVH, including  $\alpha$ 1,  $\beta$ 1 and dopamine (1-5) receptors mediated by activation of G protein receptor kinase 2 (GRK2). In experimental RVH models, chronic administration of a GRK2 inhibitor improves RV function, suggesting a potential new therapeutic target<sup>14</sup>.

$\beta$ 1-receptor downregulation in the RV may explain why PAH patients with RV failure respond so poorly to inotropes. This decreased inotropic reserve is associated with high mortality<sup>100</sup>. It appears that the adrenergic system is nearly maximally activated in RV failure<sup>14</sup>, such that catecholamine infusion may either be ineffective or perhaps actually detrimental, as in patients with LV failure<sup>101-103</sup>. In rodent RVH models, dobutamine was superior to dopamine in its ability to increase RV contractility in an RV Langendorff heart model and *in vivo*<sup>14</sup>. Mechanistically, this appeared to result from a superior coupling of dobutamine with adenylyl cyclase, evident as greater increases in cAMP occurring with dobutamine *versus* equimolar dopamine.

The choice of inotrope in RV failure is highly variable amongst PAH providers<sup>6</sup>. Based on a recent voluntary survey of practice patterns conducted on 105 experts from 25 countries with an average 11 years of experience caring for PAH patients, dobutamine was the inotropic agent of choice for managing RV failure for about 50% of providers<sup>6</sup>. This study is

limited by the voluntary nature, but does highlight the lack of standardized care received by PAH patients and highlights the need for evidence-based guidelines.

Although  $\beta$ -blockers improve outcomes in left heart failure<sup>104</sup>, they are not used clinically in PAH. That  $\beta$ -blockers might be beneficial in PAH is suggested in preclinical studies, in which PAH and RV failure are reduced by restoring the expression and sensitivity of  $\beta$ -adrenoreceptors<sup>105</sup>. However, this approach needs to be studied carefully in well-characterized patients without overt RV failure because of the potential negative inotropic effect of  $\beta$ -blockers<sup>106</sup>. Trials using carvedilol to increase RVEF in PAH are currently underway.<sup>106-108</sup>

## RV failure in PAH secondary to Congenital Heart Disease

It is worth noting that many of the features of RV failure discussed up until now, largely occur on the background of normal RV development both *in utero* and in childhood. However, in patients with RV failure and PAH secondary to congenital heart disease (CHD), there are distinguishing characteristics that require discussion and distinction. The morphologic RV in CHD may support the pulmonary circulation or the systemic circulation. RV failure may occur in several forms of CHD including right-sided obstructive lesions (tetralogy of Fallot, pulmonary atresia, double outlet RV, truncus arteriosus) or CHD with a systemic RV (transposition of great arteries palliated with the atrial switch, palliated left heart hypoplasia, congenitally corrected transposition of great arteries). RV pressure load predominates in right-sided obstructive lesions; whereas volume load is the predominant physiology in CHD with left to right shunt from atrial septal defect, pulmonary regurgitation after repair of tetralogy of Fallot repair, or tricuspid regurgitation in Ebstein's anomaly.

PAH-CHD is generally classified as (a) PAH associated with small congenital heart defects (ventricular or atrial septal defects less than 1 and 2 cm, respectively), (b) PAH associated with systemic-to-pulmonary shunts (moderate to large defects without cyanosis), (c) Eisenmenger syndrome, a right to left shunt caused by large cardiac defects (usually a ventricular septal defect). Over time this high-pressure flow causes pulmonary vascular remodeling and the rise in PVR transforms the direction of the shunt, resulting in a right to left shunt and oxygen-unresponsive hypoxemia. and (d) PAH after corrective surgery (PAH persists or recurs after surgery in the absence of residual postoperative lesions)<sup>109,110</sup>.

Increasing numbers of children with CHD survive to adulthood because of improvements in management<sup>110</sup>, so the majority of PAH-CHD patients seen in clinical practice nowadays are adults. Approximately 10% of adults with CHD develop PAH, and it is anticipated that the numbers will be increasing<sup>111</sup>. PAH predisposes to clinical deterioration and RV failure in adults with CHD, even among patients with previous defect closure and patients who had not developed Eisenmenger physiology<sup>112</sup>.

PAH-CHD carries high risk of morbidity and mortality, and the prognosis is strongly related to RV failure<sup>113</sup> and arrhythmia. PAH in adults with CHD is associated with 2-fold increase in all-cause mortality, a 3-fold higher rates of health services utilization<sup>114</sup> and an impaired quality of life<sup>114,115</sup>. With an open defect, PAH portends a 8-fold increased probability of functional limitations and this is dramatically exacerbated when Eisenmenger syndrome is

present<sup>112</sup>. Given the prevalence and adverse consequences of PAH in CHD, adults with CHD should be assessed in a tertiary setting to determine whether PAH is present.

In response to load stresses, the RV in CHD undergoes dilatation and hypertrophy, followed by changes in interventricular septal geometry, adverse ventricular-ventricular interactions and LV diastolic dysfunction. Chronic RVH leads to fibrosis and reduced contractile function. The molecular and physiological mechanisms of RV failure in response to load stresses of CHD are incompletely understood.

A large proportion of patients born with CHD in which the RV supports the systemic circulation develop RV dysfunction in early adulthood. This indicates that RV has lower capacity to support the systemic circulation as compared to the LV. Gene expression studies have shown an impaired ability of the RV to upregulate adaptive pathways to chronic hypoxia in children with CHD<sup>116</sup>. Cyanotic patients had a significantly lower expression of VEGF and glutathione peroxidase, and a higher expression of collagen compared to those who were acyanotic<sup>116</sup>. Kaufman and colleagues compared hypertrophy-signaling pathways in RV *versus* LV from patients with obstructive CHD using DNA microarrays. In RVH the transcription of adaptive remodeling pathways is lower and expression of maladaptive factors (fibroblast growth factors, transforming growth factor- $\beta$ , caspases and ubiquitin) is higher, which may explain the lower ability of the RV to adapt to hemodynamic load in CHD<sup>117</sup>. Gene expression changes have also been characterized in murine models of RV volume overload failure, and consisted of early mitochondrial bioenergetic dysfunction, enhanced TGF- $\beta$  signaling, extracellular matrix remodeling and apoptosis<sup>118</sup>. Others have shown that in isolated RV pressure load, adverse ventricular-ventricular interactions lead to LV and RV fibrosis and apoptosis, mediated through the TGF- $\beta$ 1, connective tissue growth factor and endothelin-1 pathways<sup>119</sup>.

Reddy and colleagues have described the dynamic changes in microRNA (miR) expression in a murine model of RVH and failure. The miR expression was altered, with gene targets associated with cardiomyocyte survival and growth during RVH (miR 199a-3p), and reactivation of the fetal gene program during RV failure (miR-208b). The transition from hypertrophy to failure was characterized by apoptosis and fibrosis (miR-34, -21, -1). Though most of these changes were similar to that in LV hypertrophy and failure, four miRs (-34a, -28, -148a, and -93) are upregulated in RVH/failure that were downregulated or unchanged in LVH/failure<sup>120</sup>.

Comparisons of RV tissues from animal models of PAH demonstrated upregulation of Mef2 in compensated tissues and downregulation in the decompensated RV, with inhibition of Mef2 playing a role in the transition from compensated to the decompensated RV<sup>121</sup>. Myocyte enhancer factor 2 (Mef2) is regulated by miR-208 and has also been implicated in RV gene regulation, including in a PAH model<sup>121</sup>. Additionally, miR-17, -21 and -92a have been implicated in maladaptive remodeling of the RV and pulmonary arteries in PAH. Inhibition of miR-17 and -21 in a mouse model induces a decrease in RVSP, while inhibition of all 3 miRs produces decreases in pulmonary artery muscularization<sup>122</sup>. The inhibition of miR-17 alone reduces hypoxia induced RV hypertrophy<sup>122</sup>. Knockdown of miR-21 in glioblastoma results in increased apoptotic cascade, suggesting miR-21

upregulation is a key part of the anti-apoptotic pathway seen in both malignancy and upregulated in the PAH<sup>123,124</sup>. miR are promising therapeutic targets in PAH and antagomirs of these gene regulatory molecules may be beneficial in a treatment model focused on preventing or treating pulmonary endothelial and smooth muscles cell proliferation.

Thus, in CHD, the adaptive mechanisms of the RV to stress might differ from those of the LV. Furthermore, in mice, negative inotropic response of RV myocardium to  $\alpha_1$ -adrenergic receptor stimulation in non-failing hearts becomes switched to a positive inotropic response in failing hearts. This switch mechanism involved increased myofilament  $\text{Ca}^{2+}$  sensitivity in the failing RV and may be a factor that helps the failing RV to adapt<sup>125</sup>. Similar to the LV, alterations in ubiquitin-proteasome signaling and reduced proteasome activity was seen in RVH and RV failure<sup>126</sup>. The development of RVH is associated with septal and LV apoptosis, pathological LV remodeling, and reduced LV capillary density<sup>127</sup>. Consequently, RVH causes LV diastolic dysfunction by exerting both mechanical and molecular effects on the septum and the LV myocardium.

Further work is required to delineate how the differences between RV failure from PAH and RV failure from CHD-PAH can be therapeutically exploited to improve prognosis for all patients in decompensated RV failure.

## Conclusion

RV failure in PAH has a high mortality. The maladaptive features of the RV in PAH include cancer-like changes in metabolism, dysregulated autonomic signaling, RV fibrosis and macro- and microvascular ischemia. These RV abnormalities offer new potential therapeutic targets for the management of PAH.

## Supplementary Material

Refer to Web version on PubMed Central for supplementary material.

## References

1. Hoeper MM, Bogaard HJ, Condliffe R, et al. Definitions and diagnosis of pulmonary hypertension. *Journal of the American College of Cardiology*. 2013; 62(25 Suppl):D42–50. [PubMed: 24355641]
2. Ryan JJ, Archer SL. The right ventricle in pulmonary arterial hypertension: disorders of metabolism, angiogenesis and adrenergic signaling in right ventricular failure. *Circulation research*. 2014; 115(1):176–188. [PubMed: 24951766]
3. McLaughlin VV, Archer SL, Badesch DB, et al. ACCF/AHA 2009 expert consensus document on pulmonary hypertension: a report of the American College of Cardiology Foundation Task Force on Expert Consensus Documents and the American Heart Association: developed in collaboration with the American College of Chest Physicians, American Thoracic Society, Inc., and the Pulmonary Hypertension Association. *Circulation*. 2009; 119(16):2250–2294. [PubMed: 19332472]
4. D'Alonzo GE, Barst RJ, Ayres SM, et al. Survival in patients with primary pulmonary hypertension. Results from a national prospective registry. *Annals of internal medicine*. 1991; 115(5):343–349. [PubMed: 1863023]
5. Campo A, Mathai SC, Le Pavec J, et al. Outcomes of hospitalisation for right heart failure in pulmonary arterial hypertension. *The European respiratory journal*. 2011; 38(2):359–367. [PubMed: 21310884]

6. Ryan JJ, Butrous G, Maron BA. The Heterogeneity of Clinical Practice Patterns among an International Cohort of Pulmonary Arterial Hypertension Experts. *Pulmonary circulation*. 2014; 4(3):441–451. <http://www.jstor.org/stable/10.1086/677357>. [PubMed: 25621157]
7. <http://clinicaltrials.gov/show/NCT01777607>.
8. Mehra MR, Park MH, Landzberg MJ, Lala A, Waxman AB. International Right Heart Failure Foundation Scientific Working Group. Right heart failure: toward a common language. *The Journal of heart and lung transplantation: the official publication of the International Society for Heart Transplantation*. 2014; 33(2):123–126.
9. Voelkel NF, Quaife RA, Leinwand LA, et al. Right ventricular function and failure: report of a National Heart, Lung, and Blood Institute working group on cellular and molecular mechanisms of right heart failure. *Circulation*. 2006; 114(17):1883–1891. [PubMed: 17060398]
10. Naeije R, Vachiery JL, Yerly P, Vanderpool R. The transpulmonary pressure gradient for the diagnosis of pulmonary vascular disease. *The European respiratory journal*. 2013; 41(1):217–223. [PubMed: 22936712]
11. Bogaard HJ, Abe K, Vonk Noordegraaf A, Voelkel NF. The right ventricle under pressure: cellular and molecular mechanisms of right-heart failure in pulmonary hypertension. *Chest*. 2009; 135(3):794–804. [PubMed: 19265089]
12. Piao L, Fang YH, Parikh K, Ryan JJ, Toth PT, Archer SL. Cardiac glutaminolysis: a maladaptive cancer metabolism pathway in the right ventricle in pulmonary hypertension. *Journal of molecular medicine*. 2013; 91(10):1185–1197. [PubMed: 23794090]
13. Rich S, Pogoriler J, Husain AN, Toth PT, Gomberg-Maitland M, Archer SL. Long-term effects of epoprostenol on the pulmonary vasculature in idiopathic pulmonary arterial hypertension. *Chest*. 2010; 138(5):1234–1239. [PubMed: 21051399]
14. Piao L, Fang YH, Parikh KS, et al. GRK2-mediated inhibition of adrenergic and dopaminergic signaling in right ventricular hypertrophy: therapeutic implications in pulmonary hypertension. *Circulation*. 2012; 126(24):2859–2869. [PubMed: 23124027]
15. van de Veerdonk MC, Kind T, Marcus JT, et al. Progressive right ventricular dysfunction in patients with pulmonary arterial hypertension responding to therapy. *Journal of the American College of Cardiology*. 2011; 58(24):2511–2519. [PubMed: 22133851]
16. Vonk-Noordegraaf A, Haddad F, Chin KM, et al. Right heart adaptation to pulmonary arterial hypertension: physiology and pathobiology. *Journal of the American College of Cardiology*. 2013; 62(25 Suppl):D22–33. [PubMed: 24355638]
17. Benza RL, Miller DP, Gomberg-Maitland M, et al. Predicting survival in pulmonary arterial hypertension: insights from the Registry to Evaluate Early and Long-Term Pulmonary Arterial Hypertension Disease Management (REVEAL). *Circulation*. 2010; 122(2):164–172. [PubMed: 20585012]
18. Tongers J, Schwerdtfeger B, Klein G, et al. Incidence and clinical relevance of supraventricular tachyarrhythmias in pulmonary hypertension. *American heart journal*. 2007; 153(1):127–132. [PubMed: 17174650]
19. Matthews JC, McLaughlin V. Acute right ventricular failure in the setting of acute pulmonary embolism or chronic pulmonary hypertension: a detailed review of the pathophysiology, diagnosis, and management. *Current cardiology reviews*. 2008; 4(1):49–59. [PubMed: 19924277]
20. Rubin LJ, Badesch DB. Evaluation and management of the patient with pulmonary arterial hypertension. *Annals of internal medicine*. 2005; 143(4):282–292. [PubMed: 16103472]
21. Rivero-Carvalho J. Signo para el diagnóstico de las insuficiencias tricuspideas. *Archivos del Instituto de cardiología de Mexico*. 1946; (16):531. [PubMed: 20249708]
22. Steel G. The murmur of high-pressure in the pulmonary artery. *Medical Chronicle*. 1888; (9):182.
23. Cook DJ, Simel DL. The Rational Clinical Examination. Does this patient have abnormal central venous pressure? *Jama*. 1996; 275(8):630–634. [PubMed: 8594245]
24. Sanz J, Conroy J, Narula J. Imaging of the right ventricle. *Cardiology clinics*. 2012; 30(2):189–203. [PubMed: 22548811]
25. Addetia K, Bhave NM, Tabit CE, et al. Sample size and cost analysis for pulmonary arterial hypertension drug trials using various imaging modalities to assess right ventricular size and

- function end points. *Circulation. Cardiovascular imaging*. 2014; 7(1):115–124. [PubMed: 24192452]
26. Rudski LG, Lai WW, Afilalo J, et al. Guidelines for the echocardiographic assessment of the right heart in adults: a report from the American Society of Echocardiography endorsed by the European Association of Echocardiography, a registered branch of the European Society of Cardiology, and the Canadian Society of Echocardiography. *Journal of the American Society of Echocardiography: official publication of the American Society of Echocardiography*. 2010; 23(7): 685–713. quiz 786–688. [PubMed: 20620859]
  27. Ghio S, Klersy C, Magrini G, et al. Prognostic relevance of the echocardiographic assessment of right ventricular function in patients with idiopathic pulmonary arterial hypertension. *International journal of cardiology*. 2010; 140(3):272–278. [PubMed: 19070379]
  28. Simon MA, Pinsky MR. Right ventricular dysfunction and failure in chronic pressure overload. *Cardiology research and practice*. 2011; 2011:568095. [PubMed: 21559218]
  29. Forfia PR, Fisher MR, Mathai SC, et al. Tricuspid annular displacement predicts survival in pulmonary hypertension. *American journal of respiratory and critical care medicine*. 2006; 174(9): 1034–1041. [PubMed: 16888289]
  30. Champion HC, Michelakis ED, Hassoun PM. Comprehensive invasive and noninvasive approach to the right ventricle-pulmonary circulation unit: state of the art and clinical and research implications. *Circulation*. 2009; 120(11):992–1007. [PubMed: 19752350]
  31. Fukuda Y, Tanaka H, Sugiyama D, et al. Utility of right ventricular free wall speckle-tracking strain for evaluation of right ventricular performance in patients with pulmonary hypertension. *Journal of the American Society of Echocardiography: official publication of the American Society of Echocardiography*. 2011; 24(10):1101–1108. [PubMed: 21775102]
  32. Meris A, Faletra F, Conca C, et al. Timing and magnitude of regional right ventricular function: a speckle tracking-derived strain study of normal subjects and patients with right ventricular dysfunction. *Journal of the American Society of Echocardiography: official publication of the American Society of Echocardiography*. 2010; 23(8):823–831. [PubMed: 20646910]
  33. Sachdev A, Villarraga HR, Frantz RP, et al. Right ventricular strain for prediction of survival in patients with pulmonary arterial hypertension. *Chest*. 2011; 139(6):1299–1309. [PubMed: 21148241]
  34. Pirat B, McCulloch ML, Zoghbi WA. Evaluation of global and regional right ventricular systolic function in patients with pulmonary hypertension using a novel speckle tracking method. *The American journal of cardiology*. 2006; 98(5):699–704. [PubMed: 16923465]
  35. Haeck ML, Scherptong RW, Marsan NA, et al. Prognostic value of right ventricular longitudinal peak systolic strain in patients with pulmonary hypertension. *Circulation. Cardiovascular imaging*. 2012; 5(5):628–636. [PubMed: 22875884]
  36. Benza R, Biederman R, Murali S, Gupta H. Role of cardiac magnetic resonance imaging in the management of patients with pulmonary arterial hypertension. *Journal of the American College of Cardiology*. 2008; 52(21):1683–1692. [PubMed: 19007687]
  37. Grothues F, Moon JC, Bellenger NG, Smith GS, Klein HU, Pennell DJ. Interstudy reproducibility of right ventricular volumes, function, and mass with cardiovascular magnetic resonance. *American heart journal*. 2004; 147(2):218–223. [PubMed: 14760316]
  38. van Wolferen SA, Marcus JT, Boonstra A, et al. Prognostic value of right ventricular mass, volume, and function in idiopathic pulmonary arterial hypertension. *European heart journal*. 2007; 28(10):1250–1257. [PubMed: 17242010]
  39. Swift AJ, Rajaram S, Campbell MJ, et al. Prognostic value of cardiovascular magnetic resonance imaging measurements corrected for age and sex in idiopathic pulmonary arterial hypertension. *Circulation. Cardiovascular imaging*. 2014; 7(1):100–106. [PubMed: 24275955]
  40. Freed BH, Gomberg-Maitland M, Chandra S, et al. Late gadolinium enhancement cardiovascular magnetic resonance predicts clinical worsening in patients with pulmonary hypertension. *Journal of cardiovascular magnetic resonance: official journal of the Society for Cardiovascular Magnetic Resonance*. 2012; 14:11. [PubMed: 22296860]

41. Katz J, Whang J, Boxt LM, Barst RJ. Estimation of right ventricular mass in normal subjects and in patients with primary pulmonary hypertension by nuclear magnetic resonance imaging. *Journal of the American College of Cardiology*. 1993; 21(6):1475–1481. [PubMed: 8473659]
42. Frank H, Globits S, Glogar D, Neuhold A, Kneussl M, Mlczoch J. Detection and quantification of pulmonary artery hypertension with MR imaging: results in 23 patients. *AJR. American journal of roentgenology*. 1993; 161(1):27–31. [PubMed: 8517315]
43. Dellegrottaglie S, Sanz J, Poon M, et al. Pulmonary hypertension: accuracy of detection with left ventricular septal-to-free wall curvature ratio measured at cardiac MR. *Radiology*. 2007; 243(1): 63–69. [PubMed: 17392248]
44. Vonk-Noordegraaf A, Marcus JT, Gan CT, Boonstra A, Postmus PE. Interventricular mechanical asynchrony due to right ventricular pressure overload in pulmonary hypertension plays an important role in impaired left ventricular filling. *Chest*. 2005; 128(6 Suppl):628S–630S. [PubMed: 16373882]
45. Ramani GV, Gurm G, Dilsizian V, Park MH. Noninvasive assessment of right ventricular function: will there be resurgence in radionuclide imaging techniques? *Current cardiology reports*. 2010; 12(2):162–169. [PubMed: 20425172]
46. Gaine S. Pulmonary hypertension. *Jama*. 2000; 284(24):3160–3168. [PubMed: 11135781]
47. Bilchick KC, Wise RA. Paradoxical physical findings described by Kussmaul: pulsus paradoxus and Kussmaul's sign. *Lancet*. 2002; 359(9321):1940–1942. [PubMed: 12057571]
48. Meyer TE, Sareli P, Marcus RH, Pocock W, Berk MR, McGregor M. Mechanism underlying Kussmaul's sign in chronic constrictive pericarditis. *The American journal of cardiology*. 1989; 64(16):1069–1072. [PubMed: 2816746]
49. Nadir AM, Beadle R, Lim HS. Kussmaul physiology in patients with heart failure. *Circulation. Heart failure*. 2014; 7(3):440–447. [PubMed: 24619369]
50. Ryan JJ, Rich JD, Thiruvoipati T, Swamy R, Kim GH, Rich S. Current practice for determining pulmonary capillary wedge pressure predisposes to serious errors in the classification of patients with pulmonary hypertension. *American heart journal*. 2012; 163(4):589–594. [PubMed: 22520524]
51. Kovacs G, Avian A, Pienn M, Naeije R, Olschewski H. Reading pulmonary vascular pressure tracings. How to handle the problems of zero leveling and respiratory swings. *American journal of respiratory and critical care medicine*. 2014; 190(3):252–257. [PubMed: 24869464]
52. Tedford RJ, Hassoun PM, Mathai SC, et al. Pulmonary capillary wedge pressure augments right ventricular pulsatile loading. *Circulation*. 2012; 125(2):289–297. [PubMed: 22131357]
53. Gomez A, Bialostozky D, Zajarias A, et al. Right ventricular ischemia in patients with primary pulmonary hypertension. *Journal of the American College of Cardiology*. 2001; 38(4):1137–1142. [PubMed: 11583894]
54. Vogel-Claussen J, Skrok J, Shehata ML, et al. Right and left ventricular myocardial perfusion reserves correlate with right ventricular function and pulmonary hemodynamics in patients with pulmonary arterial hypertension. *Radiology*. 2011; 258(1):119–127. [PubMed: 20971775]
55. Bian X, Fu M, Mallet RT, Bungler R, Downey HF. Myocardial oxygen consumption modulates adenosine formation by canine right ventricle in absence of hypoxia. *Journal of molecular and cellular cardiology*. 2000; 32(3):345–354. [PubMed: 10731434]
56. Voelkel NF, Gomez-Arroyo J, Abbate A, Bogaard HJ. Mechanisms of right heart failure-A work in progress and a plea for failure prevention. *Pulm Circ*. 2013; 3(1):137–143. [PubMed: 23662190]
57. Piao L, Sidhu VK, Fang YH, et al. FOXO1-mediated upregulation of pyruvate dehydrogenase kinase-4 (PDK4) decreases glucose oxidation and impairs right ventricular function in pulmonary hypertension: therapeutic benefits of dichloroacetate. *Journal of molecular medicine*. 2013; 91(3): 333–346. [PubMed: 23247844]
58. Ohira H, Beanlands RS, Davies RA, Mielniczuk L. The role of nuclear imaging in pulmonary hypertension. *Journal of nuclear cardiology: official publication of the American Society of Nuclear Cardiology*. 2014
59. Nagaya N, Nishikimi T, Uematsu M, et al. Plasma brain natriuretic peptide as a prognostic indicator in patients with primary pulmonary hypertension. *Circulation*. 2000; 102(8):865–870. [PubMed: 10952954]



60. Sakamaki F, Satoh T, Nagaya N, et al. Correlation between severity of pulmonary arterial hypertension and 123I-metaiodobenzylguanidine left ventricular imaging. *Journal of nuclear medicine: official publication, Society of Nuclear Medicine*. 2000; 41(7):1127–1133.
61. Bristow MR, Minobe W, Rasmussen R, et al. Beta-adrenergic neuroeffector abnormalities in the failing human heart are produced by local rather than systemic mechanisms. *The Journal of clinical investigation*. 1992; 89(3):803–815. [PubMed: 1311717]
62. Ujeyl A, Inada K, Hillmann K, et al. Right heart function prediction of outcome in heart failure patients after catheter ablation for recurrent ventricular tachycardia. *JACC. Heart failure*. 2013; 1(4):281–289. [PubMed: 24621931]
63. Doesch C, Dierks DM, Haghi D, et al. Right ventricular dysfunction, late gadolinium enhancement, and female gender predict poor outcome in patients with dilated cardiomyopathy. *International journal of cardiology*. 2014; 177(2):429–435. [PubMed: 25304065]
64. Grigioni F, Potena L, Galie N, et al. Prognostic implications of serial assessments of pulmonary hypertension in severe chronic heart failure. *The Journal of heart and lung transplantation: the official publication of the International Society for Heart Transplantation*. 2006; 25(10):1241–1246.
65. Puwanant S, Priester TC, Mookadam F, Bruce CJ, Redfield MM, Chandrasekaran K. Right ventricular function in patients with preserved and reduced ejection fraction heart failure. *European journal of echocardiography: the journal of the Working Group on Echocardiography of the European Society of Cardiology*. 2009; 10(6):733–737.
66. Mohammed SF, Hussain I, Abou Ezzeddine OF, et al. Right Ventricular Function in Heart Failure with Preserved Ejection Fraction: A Community Based Study. *Circulation*. 2014
67. Oosterhof T, Tulevski II, Vliegen HW, Spijkerboer AM, Mulder BJ. Effects of volume and/or pressure overload secondary to congenital heart disease (tetralogy of fallot or pulmonary stenosis) on right ventricular function using cardiovascular magnetic resonance and B-type natriuretic peptide levels. *The American journal of cardiology*. 2006; 97(7):1051–1055. [PubMed: 16563914]
68. Haddad F, Doyle R, Murphy DJ, Hunt SA. Right ventricular function in cardiovascular disease, part II: pathophysiology, clinical importance, and management of right ventricular failure. *Circulation*. 2008; 117(13):1717–1731. [PubMed: 18378625]
69. Hopkins WE, Waggoner AD. Severe pulmonary hypertension without right ventricular failure: the unique hearts of patients with Eisenmenger syndrome. *The American journal of cardiology*. 2002; 89(1):34–38. [PubMed: 11779519]
70. Kawut SM, Taichman DB, Archer-Chicko CL, Palevsky HI, Kimmel SE. Hemodynamics and survival in patients with pulmonary arterial hypertension related to systemic sclerosis. *Chest*. 2003; 123(2):344–350. [PubMed: 12576350]
71. Kuhn KP, Byrne DW, Arbogast PG, Doyle TP, Loyd JE, Robbins IM. Outcome in 91 consecutive patients with pulmonary arterial hypertension receiving epoprostenol. *American journal of respiratory and critical care medicine*. 2003; 167(4):580–586. [PubMed: 12446266]
72. Hopkins WE, Ochoa LL, Richardson GW, Trulock EP. Comparison of the hemodynamics and survival of adults with severe primary pulmonary hypertension or Eisenmenger syndrome. *The Journal of heart and lung transplantation: the official publication of the International Society for Heart Transplantation*. 1996; 15(1 Pt 1):100–105.
73. Fang YH, Piao L, Hong Z, et al. Therapeutic inhibition of fatty acid oxidation in right ventricular hypertrophy: exploiting Randle's cycle. *Journal of molecular medicine*. 2012; 90(1):31–43. [PubMed: 21874543]
74. Cavin MA, Demos-Davies K, Horn TR, et al. Selective class I histone deacetylase inhibition suppresses hypoxia-induced cardiopulmonary remodeling through an antiproliferative mechanism. *Circulation research*. 2012; 110(5):739–748. [PubMed: 22282194]
75. Zhao L, Chen CN, Hajji N, et al. Histone deacetylation inhibition in pulmonary hypertension: therapeutic potential of valproic acid and suberoylanilide hydroxamic acid. *Circulation*. 2012; 126(4):455–467. [PubMed: 22711276]
76. Bogaard HJ, Mizuno S, Hussaini AA, et al. Suppression of histone deacetylases worsens right ventricular dysfunction after pulmonary artery banding in rats. *American journal of respiratory and critical care medicine*. 2011; 183(10):1402–1410. [PubMed: 21297075]

77. Piao L, Fang YH, Cadete VJ, et al. The inhibition of pyruvate dehydrogenase kinase improves impaired cardiac function and electrical remodeling in two models of right ventricular hypertrophy: resuscitating the hibernating right ventricle. *Journal of molecular medicine*. 2010; 88(1):47–60. [PubMed: 19949938]
78. Guarracino F, Cariello C, Danella A, et al. Right ventricular failure: physiology and assessment. *Minerva Anestesiol*. 2005; 71(6):307–312. [PubMed: 15886593]
79. Archer SL, Fang YH, Ryan JJ, Piao L. Metabolism and bioenergetics in the right ventricle and pulmonary vasculature in pulmonary hypertension. *Pulm Circ*. 2013; 3(1):144–152. [PubMed: 23662191]
80. Bogaard HJ, Natarajan R, Henderson SC, et al. Chronic pulmonary artery pressure elevation is insufficient to explain right heart failure. *Circulation*. 2009; 120(20):1951–1960. [PubMed: 19884466]
81. Piao L, Fang YH, Parikh KS, Ryan JJ, Toth PT, Archer SL. Cardiac Glutaminolysis: A Maladaptive Cancer Metabolism Pathway in the Right Ventricle in Pulmonary Hypertension. *Journal of molecular medicine*. 2013 accepted for publication.
82. van Wolferen SA, Marcus JT, Westerhof N, et al. Right coronary artery flow impairment in patients with pulmonary hypertension. *European heart journal*. 2008; 29(1):120–127. [PubMed: 18065750]
83. Vlahakes GJ, Baer RW, Uhlig PN, Verrier ED, Bristow JD, Hoffmann JI. Adrenergic influence in the coronary circulation of conscious dogs during maximal vasodilation with adenosine. *Circulation research*. 1982; 51(3):371–384. [PubMed: 6126283]
84. Bian X, Williams AG Jr, Gwartz PA, Downey HF. Right coronary autoregulation in conscious, chronically instrumented dogs. *The American journal of physiology*. 1998; 275(1 Pt 2):H169–175. [PubMed: 9688910]
85. Marsboom G, Toth PT, Ryan JJ, et al. Dynamin-related protein 1-mediated mitochondrial mitotic fission permits hyperproliferation of vascular smooth muscle cells and offers a novel therapeutic target in pulmonary hypertension. *Circulation research*. 2012; 110(11):1484–1497. [PubMed: 22511751]
86. Oikawa M, Kagaya Y, Otani H, et al. Increased [18F]fluorodeoxyglucose accumulation in right ventricular free wall in patients with pulmonary hypertension and the effect of epoprostenol. *Journal of the American College of Cardiology*. 2005; 45(11):1849–1855. [PubMed: 15936618]
87. Lundgrin EL, Park MM, Sharp J, et al. Fasting 2-deoxy-2-[18F]fluoro-D-glucose positron emission tomography to detect metabolic changes in pulmonary arterial hypertension hearts over 1 year. *Annals of the American Thoracic Society*. 2013; 10(1):1–9. [PubMed: 23509326]
88. McMurtry MS, Bonnet S, Wu X, et al. Dichloroacetate prevents and reverses pulmonary hypertension by inducing pulmonary artery smooth muscle cell apoptosis. *Circulation research*. 2004; 95(8):830–840. [PubMed: 15375007]
89. Michelakis ED, McMurtry MS, Wu XC, et al. Dichloroacetate, a metabolic modulator, prevents and reverses chronic hypoxic pulmonary hypertension in rats: role of increased expression and activity of voltage-gated potassium channels. *Circulation*. 2002; 105(2):244–250. [PubMed: 11790708]
90. Piao L, Sidhu VK, Fang YH, et al. FOXO1-mediated upregulation of pyruvate dehydrogenase kinase-4 (PDK4) decreases glucose oxidation and impairs right ventricular function in pulmonary hypertension: therapeutic benefits of dichloroacetate. *J Mol Med (Berl)*. 2013; 91(3):333–346. [PubMed: 23247844]
91. <http://clinicaltrials.gov/ct2/show/NCT01083524>.
92. Randle PJ, Garland PB, Hales CN, Newsholme EA. The glucose fatty-acid cycle. Its role in insulin sensitivity and the metabolic disturbances of diabetes mellitus. *Lancet*. 1963; 1(7285):785–789. [PubMed: 13990765]
93. <http://www.clinicaltrials.gov/ct2/show/NCT01174173>.
94. NCT01174173, Last accessed November 1, 2014.
95. Dang CV. Glutaminolysis: supplying carbon or nitrogen or both for cancer cells? *Cell Cycle*. 2010; 9(19):3884–3886. [PubMed: 20948290]

96. Wise DR, Thompson CB. Glutamine addiction: a new therapeutic target in cancer. *Trends in biochemical sciences*. 2010; 35(8):427–433. [PubMed: 20570523]
97. Nootens M, Kaufmann E, Rector T, et al. Neurohormonal activation in patients with right ventricular failure from pulmonary hypertension: relation to hemodynamic variables and endothelin levels. *Journal of the American College of Cardiology*. 1995; 26(7):1581–1585. [PubMed: 7594089]
98. Brown L, Miller J, Dagger A, Sernia C. Cardiac and vascular responses after monocrotaline-induced hypertrophy in rats. *J Cardiovasc Pharmacol*. 1998; 31(1):108–115. [PubMed: 9456285]
99. Usui S, Yao A, Hatano M, et al. Upregulated neurohumoral factors are associated with left ventricular remodeling and poor prognosis in rats with monocrotaline-induced pulmonary arterial hypertension. *Circ J*. 2006; 70(9):1208–1215. [PubMed: 16936438]
100. Campo A, Mathai SC, Le Pavec J, et al. Outcomes of hospitalisation for right heart failure in pulmonary arterial hypertension. *Eur Respir J*. 2011; 38(2):359–367. [PubMed: 21310884]
101. Cohn JN, Goldstein SO, Greenberg BH, et al. Vesnarinone Trial Investigators. A dose-dependent increase in mortality with vesnarinone among patients with severe heart failure. *The New England journal of medicine*. 1998; 339(25):1810–1816. [PubMed: 9854116]
102. O'Connor CM, Gattis WA, Uretsky BF, et al. Continuous intravenous dobutamine is associated with an increased risk of death in patients with advanced heart failure: insights from the Flolan International Randomized Survival Trial (FIRST). *American heart journal*. 1999; 138(1 Pt 1):78–86. [PubMed: 10385768]
103. Packer M, Carver JR, Rodeheffer RJ, et al. The PROMISE Study Research Group. Effect of oral milrinone on mortality in severe chronic heart failure. *The New England journal of medicine*. 1991; 325(21):1468–1475. [PubMed: 1944425]
104. Chatterjee S, Udell JA, Sardar P, Lichstein E, Ryan JJ. Comparable benefit of beta-blocker therapy in heart failure across regions of the world: meta-analysis of randomized clinical trials. *The Canadian journal of cardiology*. 2014; 30(8):898–903. [PubMed: 24939477]
105. Tual L, Morel OE, Favret F, et al. Carvedilol inhibits right ventricular hypertrophy induced by chronic hypobaric hypoxia. *Pflugers Arch*. 2006; 452(4):371–379. [PubMed: 16639551]
106. Grinnan D, Bogaard HJ, Grizzard J, et al. Treatment of group I pulmonary arterial hypertension with carvedilol is safe. *American journal of respiratory and critical care medicine*. 2014; 189(12):1562–1564. [PubMed: 24930531]
107. <http://clinicaltrials.gov/show/NCT02120339>.
108. <http://clinicaltrials.gov/ct2/show/NCT01586156>.
109. Gupta V, Tonelli AR, Krasuski RA. Congenital heart disease and pulmonary hypertension. *Heart failure clinics*. 2012; 8(3):427–445. [PubMed: 22748904]
110. Simonneau G, Gatzoulis MA, Adatia I, et al. Updated clinical classification of pulmonary hypertension. *Journal of the American College of Cardiology*. 2013; 62(25 Suppl):D34–41. [PubMed: 24355639]
111. Marelli AJ, Mackie AS, Ionescu-Ittu R, Rahme E, Pilote L. Congenital heart disease in the general population: changing prevalence and age distribution. *Circulation*. 2007; 115(2):163–172. [PubMed: 17210844]
112. Engelfriet PM, Duffels MG, Moller T, et al. Pulmonary arterial hypertension in adults born with a heart septal defect: the Euro Heart Survey on adult congenital heart disease. *Heart*. 2007; 93(6):682–687. [PubMed: 17164490]
113. Ghio S, Gavazzi A, Campana C, et al. Independent and additive prognostic value of right ventricular systolic function and pulmonary artery pressure in patients with chronic heart failure. *Journal of the American College of Cardiology*. 2001; 37(1):183–188. [PubMed: 11153735]
114. Lowe BS, Therrien J, Ionescu-Ittu R, Pilote L, Martucci G, Marelli AJ. Diagnosis of pulmonary hypertension in the congenital heart disease adult population impact on outcomes. *Journal of the American College of Cardiology*. 2011; 58(5):538–546. [PubMed: 2177753]
115. Duffels MG, Engelfriet PM, Berger RM, et al. Pulmonary arterial hypertension in congenital heart disease: an epidemiologic perspective from a Dutch registry. *International journal of cardiology*. 2007; 120(2):198–204. [PubMed: 17182132]

116. Reddy S, Osorio JC, Duque AM, et al. Failure of right ventricular adaptation in children with tetralogy of Fallot. *Circulation*. 2006; 114(1 Suppl):I37–42. [PubMed: 16820602]
117. Kaufman BD, Desai M, Reddy S, et al. Genomic profiling of left and right ventricular hypertrophy in congenital heart disease. *Journal of cardiac failure*. 2008; 14(9):760–767. [PubMed: 18995181]
118. Reddy S, Zhao M, Hu DQ, et al. Physiologic and molecular characterization of a murine model of right ventricular volume overload. *American journal of physiology. Heart and circulatory physiology*. 2013; 304(10):H1314–1327. [PubMed: 23504182]
119. Friedberg MK, Cho MY, Li J, et al. Adverse biventricular remodeling in isolated right ventricular hypertension is mediated by increased transforming growth factor-beta1 signaling and is abrogated by angiotensin receptor blockade. *American journal of respiratory cell and molecular biology*. 2013; 49(6):1019–1028. [PubMed: 23841477]
120. Reddy S, Zhao M, Hu DQ, et al. Dynamic microRNA expression during the transition from right ventricular hypertrophy to failure. *Physiological genomics*. 2012; 44(10):562–575. [PubMed: 22454450]
121. Paulin R, Sutendra G, Gurtu V, et al. A miR-208-Mef2 Axis Drives the De-Compensation of Right Ventricular Function in Pulmonary Hypertension. *Circulation research*. 2014
122. Pullamsetti SS, Doebele C, Fischer A, et al. Inhibition of microRNA-17 improves lung and heart function in experimental pulmonary hypertension. *American journal of respiratory and critical care medicine*. 2012; 185(4):409–419. [PubMed: 22161164]
123. Chan JA, Krichevsky AM, Kosik KS. MicroRNA-21 is an antiapoptotic factor in human glioblastoma cells. *Cancer research*. 2005; 65(14):6029–6033. [PubMed: 16024602]
124. Sarkar J, Gou D, Turaka P, Viktorova E, Ramchandran R, Raj JU. MicroRNA-21 plays a role in hypoxia-mediated pulmonary artery smooth muscle cell proliferation and migration. *American journal of physiology. Lung cellular and molecular physiology*. 2010; 299(6):L861–871. [PubMed: 20693317]
125. Wang GY, Yeh CC, Jensen BC, Mann MJ, Simpson PC, Baker AJ. Heart failure switches the RV alpha1-adrenergic inotropic response from negative to positive. *American journal of physiology. Heart and circulatory physiology*. 2010; 298(3):H913–920. [PubMed: 20035030]
126. Rajagopalan V, Zhao M, Reddy S, et al. Altered ubiquitin-proteasome signaling in right ventricular hypertrophy and failure. *American journal of physiology. Heart and circulatory physiology*. 2013; 305(4):H551–562. [PubMed: 23729213]
127. Kitahori K, He H, Kawata M, et al. Development of left ventricular diastolic dysfunction with preservation of ejection fraction during progression of infant right ventricular hypertrophy. *Circulation. Heart failure*. 2009; 2(6):599–607. [PubMed: 19919985]
128. Yeo TC, Dujardin KS, Tei C, Mahoney DW, McGoon MD, Seward JB. Value of a Doppler-derived index combining systolic and diastolic time intervals in predicting outcome in primary pulmonary hypertension. *The American journal of cardiology*. 1998; 81(9):1157–1161. [PubMed: 9605059]
129. Mauritz GJ, Kind T, Marcus JT, et al. Progressive changes in right ventricular geometric shortening and long-term survival in pulmonary arterial hypertension. *Chest*. 2012; 141(4):935–943. [PubMed: 21960697]
130. Michelakis ED, Tymchak W, Noga M, et al. Long-term treatment with oral sildenafil is safe and improves functional capacity and hemodynamics in patients with pulmonary arterial hypertension. *Circulation*. 2003; 108(17):2066–2069. [PubMed: 14568893]
131. Marrone G, Mamone G, Luca A, et al. The role of 1.5T cardiac MRI in the diagnosis, prognosis and management of pulmonary arterial hypertension. *The international journal of cardiovascular imaging*. 2010; 26(6):665–681. [PubMed: 20336377]
132. van Wolferen SA, van de Veerdonk MC, Mauritz GJ, et al. Clinically significant change in stroke volume in pulmonary hypertension. *Chest*. 2011; 139(5):1003–1009. [PubMed: 20864614]
133. Carrio I. Cardiac neurotransmission imaging. *Journal of nuclear medicine: official publication, Society of Nuclear Medicine*. 2001; 42(7):1062–1076.

134. Marsboom G, Wietholt C, Haney CR, et al. Lung (1)(8)F-fluorodeoxyglucose positron emission tomography for diagnosis and monitoring of pulmonary arterial hypertension. *American journal of respiratory and critical care medicine*. 2012; 185(6):670–679. [PubMed: 22246173]
135. Hagan G, Southwood M, Treacy C, et al. (18)FDG PET imaging can quantify increased cellular metabolism in pulmonary arterial hypertension: A proof-of-principle study. *Pulm Circ*. 2011; 1(4):448–455. [PubMed: 22530099]
136. McMurtry MS, Bonnet S, Wu X, et al. Dichloroacetate prevents and reverses pulmonary hypertension by inducing pulmonary artery smooth muscle cell apoptosis. *Circulation research*. 2004; 95(8):830–840. [PubMed: 15375007]

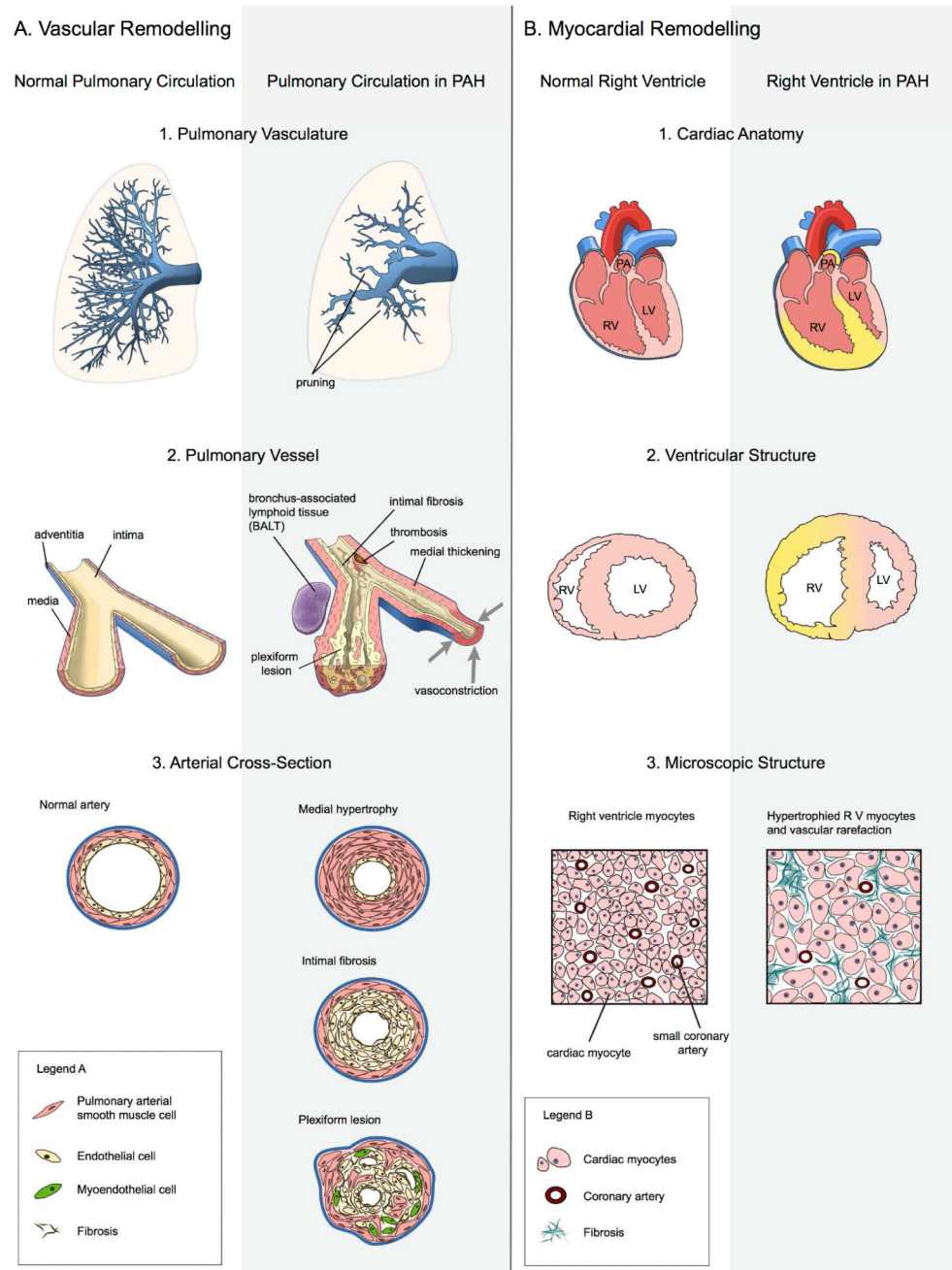


**Figure 1. Right ventricular failure in Pulmonary Arterial Hypertension**

The Pulmonary Arterial Hypertension Phenotype: An obstructed vascular bed resulting in a hypertrophied dilated, right ventricle. Left hand images: Pulmonary arteries (PAs) become “pruned” in PAH. PAs develop medial hypertrophy, intimal fibrosis, vasoconstriction and inflammation in the adventitia, which causes severe luminal obstruction in PAH, compared to control.

Right hand images: Right ventricle in normal individual is thin and small, compared with hypertrophied, fibrotic, ischemic, remodeled right ventricle in PAH.

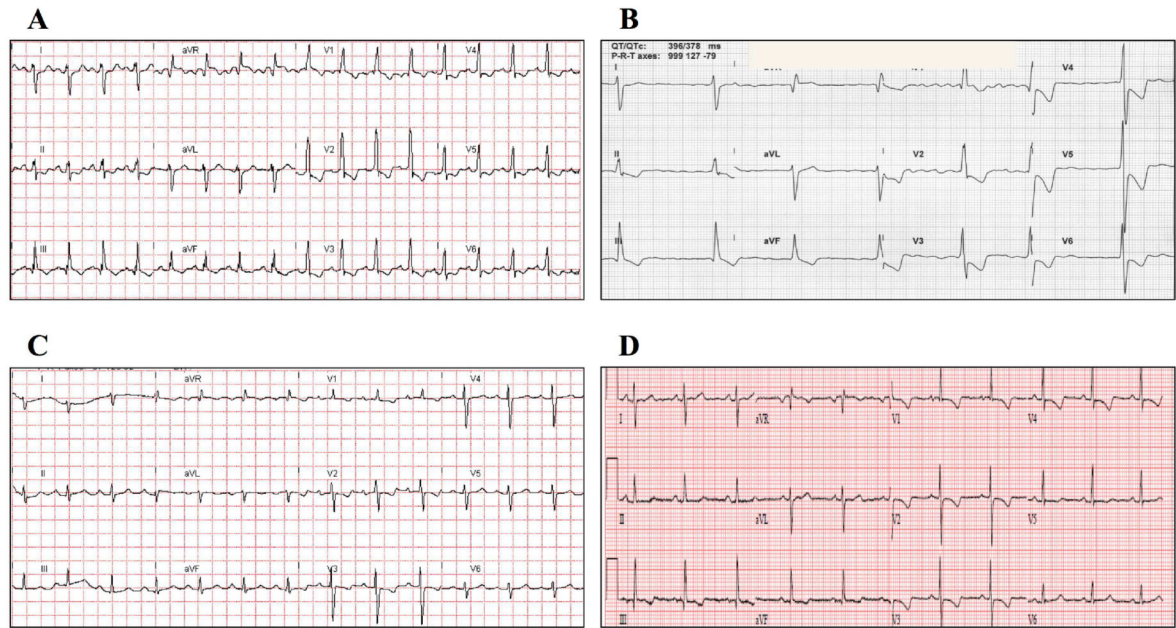


**Figure 2. Electrocardiogram of patients with PAH**

ECG in patients with PAH frequently shows (A) right bundle branch block; (B) prominent R wave and ST depression across the precordium; (C) right axis deviation; and (D)  $S_1Q_3T_3$  pattern.

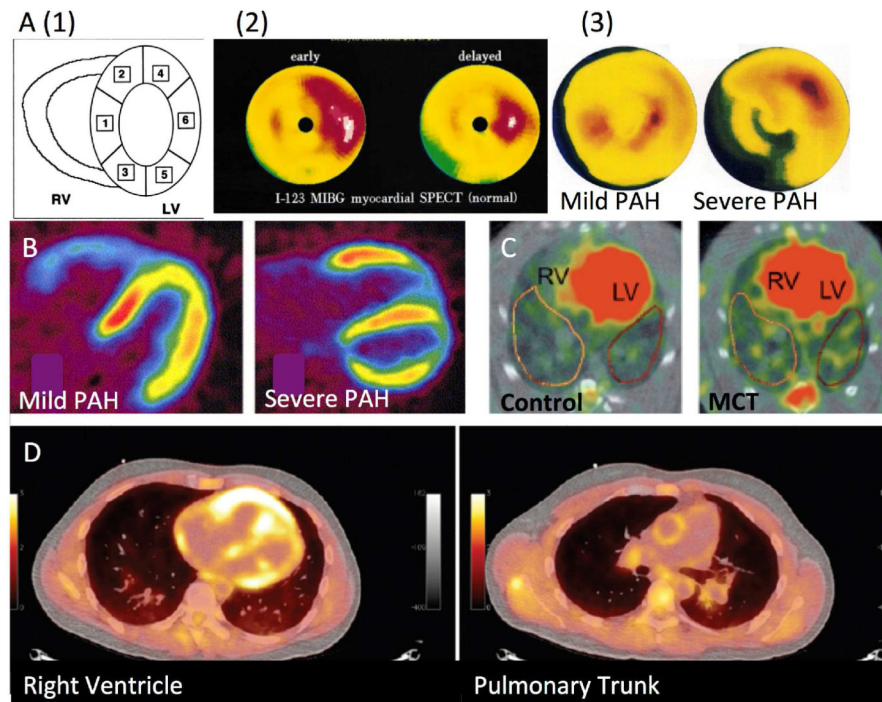


### Figure 3. Nuclear Assessment of the Right Ventricle

(A)(1) Diagram of MIBG images<sup>60</sup>, MIBG Uptake in the LV in (2) a healthy volunteer<sup>133</sup> and (3) PH patients, a patient with mild Group1 PH (mPAP 22mmHg) and a patient with severe Group 1 PH (mPAP 77mmHg)<sup>60</sup>. In this image decreased myocardial MIBG uptake in is shown as green or blue color in region of interventricular septum in both patients and in inferior LV wall in the severe PH patient<sup>60</sup>.

(B) Increased <sup>18</sup>F-FDG in the RV of PAH patients on epoprostenol. FDG-PET images of patients with mild (A, mean pulmonary artery pressure, 33 mm Hg) and severe pulmonary hypertension (B, mean pulmonary artery pressure, 81 mm Hg)<sup>86</sup>. (C) PET showing Increased <sup>18</sup>F-fluorodeoxyglucose(FDG) uptake in RV and lung in monocrotaline (MCT) animal<sup>134</sup>. (D) Fused PET/CT of RV and pulmonary trunk in an iPAH patient<sup>135</sup>.



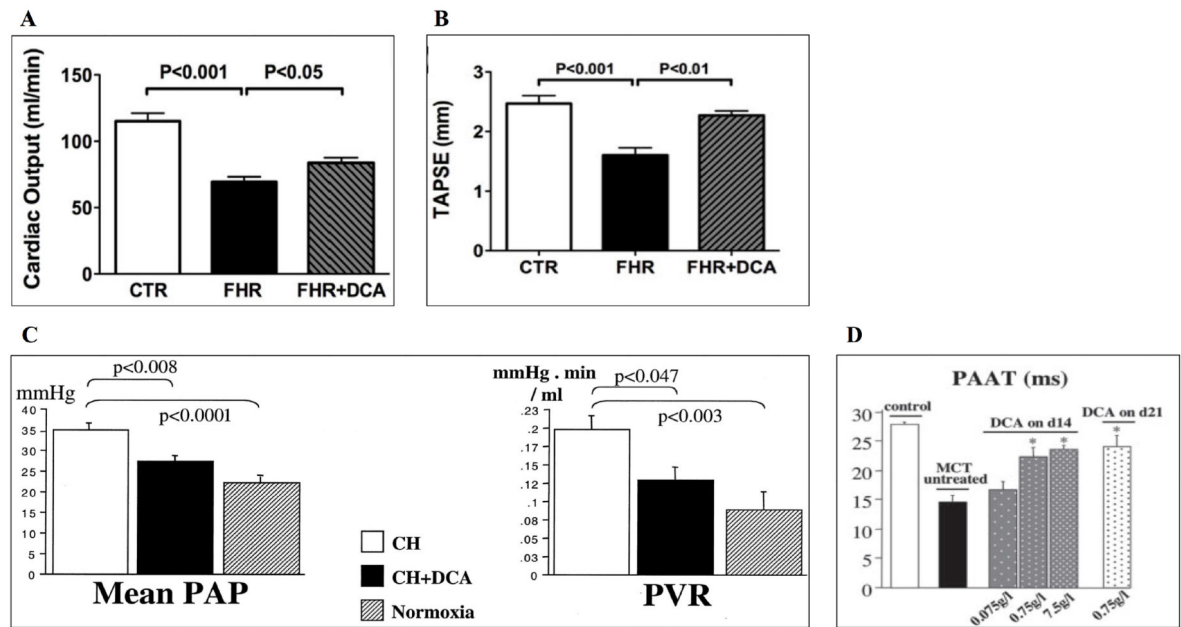


**Figure 4. Metabolic Treatment of Animal Models of PAH with Dichloroacetate**  
 Dichloroacetate (DCA) has demonstrated hemodynamic effects in animal models of pulmonary arterial hypertension (PAH): (A & B) Fawn-hood rat (FHR) model of PAH: DCA increases cardiac output and RV function (TAPSE). (C) Chronic hypoxic model of PAH: DCA decreases mean pulmonary artery pressure and pulmonary vascular resistance. (D) Monocrotaline model of PAH: DCA prolongs in pulmonary artery acceleration time, reflective of a decrease in pulmonary vascular resistance. Reproduced with permission from <sup>57,89,136</sup>.

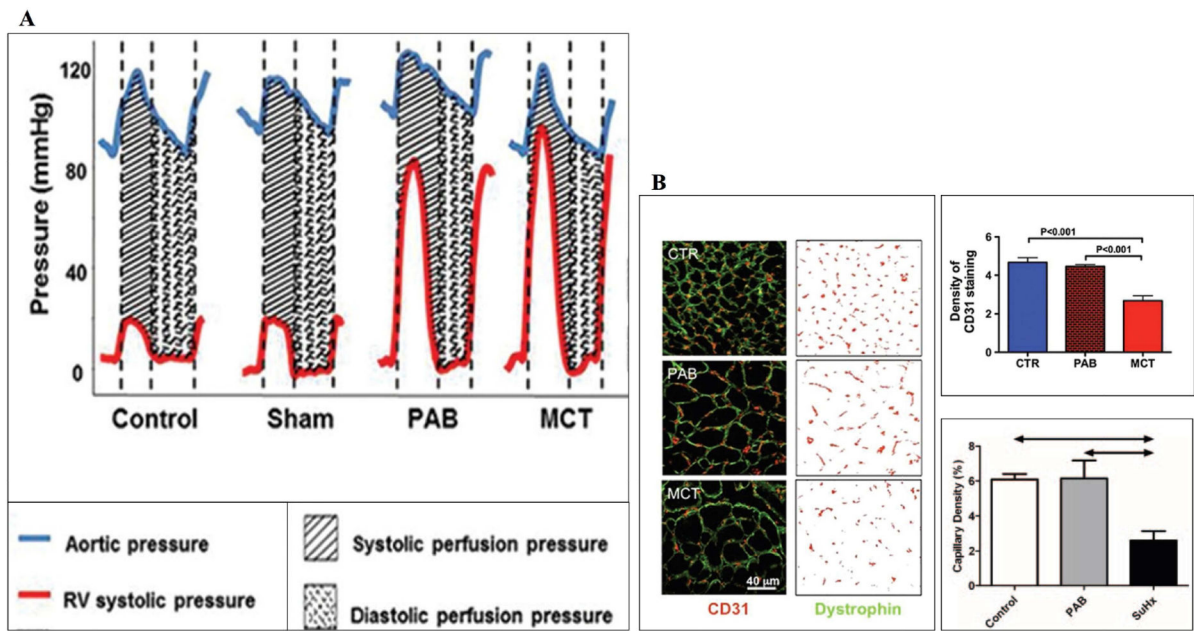


**Figure 5. Mechanisms of Right ventricular ischemia in PAH**

(A) Coronary artery perfusion pressure is reduced in both pulmonary artery banding (PAB) and monocrotaline (MCT) models. (B) Right ventricular capillary density is reduced in both MCT and Chronic Hypoxia-Sugen (SuHx) models, but not in PAB model. Dystrophin is labeled green, marking myocyte membranes. Both dystrophin and CD31 (in red) are shown in the left column of panel B. CD31 only is shown in the right panel. The red circles are CD31 positive endothelial cells showing the loss of microvascular bed in monocrotaline RVs. Reproduced with permission from <sup>11,79</sup>.

**Table 1**  
**Clinical features of right ventricular failure**

Symptomology	Signs	Diagnostic Testing
Dyspnea on Exertion Lower Extremity Swelling Palpitations Fatigue Generalized Weakness Abdominal Fullness Pre-syncope Syncope	Distended Neck Veins Tricuspid regurgitation murmur Peripheral Edema Hepatomegaly RV Heave Rights sided third hear sound (S3) Hepatojugular reflex Kussmaul's sign	Reduced renal function Hyponatremia EKG Abnormalities <ul style="list-style-type: none"> <li>- Right axis deviation</li> <li>- Prominent precordial R waves</li> </ul> Right ventricular strain <ul style="list-style-type: none"> <li>- Incomplete RBBB</li> </ul> Chest X-Ray <ul style="list-style-type: none"> <li>- Cardiomegaly Echocardiography</li> <li>- Right atrial dilation</li> <li>- Right ventricle dilation</li> <li>- Reduced right ventricular EF</li> </ul> Heart Catheterization <ul style="list-style-type: none"> <li>- Reduced cardiac index</li> <li>- Increased RV filling pressure</li> </ul>

Author Manuscript

Author Manuscript

Author Manuscript

Author Manuscript

**Table 2**  
**Echocardiographic Right Ventricular Parameters Significantly Correlated with Mortality in PH**

Echocardiographic Method	Echo View	Parameter indicating RV dysfunction	Prognosis		
TAPSE	Apical 4-CH <ul style="list-style-type: none"> <li>m-mode of lateral tricuspid annulus</li> </ul>	< 18 mm	TAPSE < 18 mm associated with increased RV dysfunction, increased 1 and 2 yr mortality. Hazard ratio of 5.7 <sup>29</sup> .		
Tei Index (also known as RV-MPI)	Apical 4-CH <ul style="list-style-type: none"> <li>Pulse Doppler of TR regurgitation</li> <li>Tissue Doppler of lateral tricuspid annulus</li> </ul>	>0.40 by Pulse Doppler > 0.55 by Tissue Doppler	5 year survival (free of death or lung transplantation):		
			Tei index	5 yr survival	
			<0.83	74%	
			0.83	4%	
			Hazard ratio of 1.3 for every 0.1 unit increase in Tei index <sup>128</sup> .		
Peak systolic tricuspid lateral annular velocity (S')	Pulse Doppler tissue imaging (DTI) of the tricuspid annulus	< 9.7 cm/sec	<9.7 cm/sec associated with abnormal RV contractility <sup>30</sup> .		
RV fractional area change (= [End-diastolic area] - [End-systolic area] / End-diastolic area)	Apical 4-CH	< 35%	RVFAC significantly higher in 4 year survivors vs. nonsurvivors, (31%±9 vs. 24%±10) <sup>129</sup> .		
Speckle Tracking Longitudinal Peak Systolic Strain (RV LPSS)	Apical 4-CH	<u>More negative than (&gt;)-19%</u>	Survival rates (%)		
			Yr	> -19% (higher strain)	≤ -19% (lower strain)
			1	93	77
			3	90	66
			5	90	55
			1% decrease (more negative) in LPSS = 13% increased risk of death. <sup>35</sup>		

IVA, isovolumic acceleration; IVCv, isovolumic contraction velocity; MPI, myocardial performance index; RAP, right atrial pressure; RV, right ventricle; TAPSE, tricuspid annular plane systolic excursion; DTI, Doppler tissue imaging; TR, tricuspid regurgitation; 4CH, four chamber view; AS, Area Strain

**Table 3**  
**MRI Features of Right Ventricular Adaptation and Failure**

Feature	Significance	Parameter indicating RV dysfunction	Prognostics
RV mass	Increased mass correlates with mPAP. Mass decreases in response to sildenafil therapy <sup>30, 130</sup> .		Non-significant trend towards increased mortality.
RV end diastolic volume index (RVEDVI)	Dilatation and increased volume signifies a progression of RV pressure overload.	84mL/m	Associated with increased mortality <sup>38</sup> .
RV Ejection Fraction (RVEF).	Better mortality prediction than PVR <sup>15</sup> . Increased in response to sildenafil therapy <sup>130</sup> .	<35%	Increased mortality is independent of baseline PVR and PVR change with therapy <sup>15</sup> .
RV longitudinal shortening	TAPSE measurement equivalent <sup>15</sup> .	<15 mm	Non-survivors had reduced longitudinal shortening (14+7mm vs. 20+5mm) <sup>129</sup> .
RV transverse shortening	Incorporates free wall and septal movements <sup>129</sup> .		Non-survivors had reduced shortening in segments 2-7.
RV Fractional area change (RV FAC)	Used as a surrogate for ejection fraction	< 24%	Non-survivors <ul style="list-style-type: none"> <li>- decreased at baseline (24%±10 vs. 31%±9)</li> <li>- 1 year follow-up decreased by 17%±10<sup>129</sup>.</li> </ul>
LV end diastolic volume	Decreased with septal bowing with impaired LV filling	40 mL/m	Increased mortality <sup>238</sup> .
Left ventricular septal-to-free-wall curvature ratio	Used to estimate RVSP, objective measurement of septal bowing into the LV <sup>131</sup> .	Ratio >0.67	87% sensitivity, 100% specificity for elevated RVSP <sup>43</sup> .
LV Stroke Volume Index (LV SVI)	Normal SV indicates RV adapted to increased afterload - 10mL changes in SV are	LV SVI 25mL/m	Increased mortality <sup>238</sup> .

Feature	Significance	Parameter indicating RV dysfunction	Prognostics
	significant, <sup>1,32</sup>		

Author Manuscript

Author Manuscript

Author Manuscript

Author Manuscript